
Water Electrolysis with Inductive Voltage Pulses

Martins Vanags, Janis Kleperis and Gunars Bajars

Additional information is available at the end of the chapter

<http://dx.doi.org/10.5772/52453>

1. Introduction

The main idea of Hydrogen Economy is to create a bridge between the energy resources, energy producers and consumers. If hydrogen is produced from renewable energy sources (wind, solar, hydro, biomass, etc.), and used for energy production in the catalytic combustion process, then the energy life cycle does not pollute nature longer. With transition to Hydrogen Economy the Society will live accordingly to the sustainable development model, defined in the 1987 (Our Common Future, 1987).

Hydrogen is not available on Earth in free form; therefore the production process is representing a major part of the final price of hydrogen (Hydrogen Pathway, 2011). This is the main reason while research for effective electrolysis methods is very urgent. On our Planet the hydrogen is mainly located in compounds such as hydrocarbons, water, etc. and appropriate energy is needed to release hydrogen from them. In principle the amount of consumed energy is always greater than that which can be extracted from the hydrogen, and in the real operating conditions, the cycle efficiency does not exceed 50% (The Hydrogen Economy, 2004). The current problem is motivated to seek improvements to existing and discovering new technologies to produce hydrogen from the water – widely available and renewable resource on the Earth.

Water electrolysis is known more than 130 years already, and different technologies are developed giving power consumption around 3.6 kWh/m³ - high temperature electrolysis, and 4.1 kWh/m³ - room temperature alkaline electrolyzers and proton exchange membrane electrolyzers (The Hydrogen Economy, 2004). Lower hydrogen production costs is for technologies using closed thermo-chemical cycles, but only in places where huge amount of waste heat is available (for example, nuclear power stations (The Hydrogen Economy, 2004). Nevertheless what will be the hydrogen price today, in future only hydrogen obtained from renewable resources using electricity from renewable energy sources will save the World, as

it was stated in 2nd World's Hydrogen Congress in Turkey (Selected Articles, 2009). For Latvia the hydrogen obtained in electrolysis using electricity from renewables (wind, Sun, water) also would be the best solution to move to Hydrogen Economics (Dimants et al, 2011). That is because all renewables available in Latvia's geographical situation are giving non-stable and interrupt power, for which the storage solutions are necessary. Usage of hydrogen as energy carrier to be produced from electricity generated by renewables, stored and after used in fuel cell stack to generate electricity is the best solution (Zoulias, 2002). Efficient and stable electrolyzers are required for such purposes. Smaller electrolysis units are necessary also for technical solutions where hydrogen is produced and used directly on demand, for example, hydrogen welding devices, hydrogen powered internal combustion cars (Kreuter and Hofmann, 1998).

DC power typically is used for electrolysis, nevertheless pulse powering also is proposed (see, for example, Guttmann and Murphy, 1983). Using a mechanically interrupted DC power supply (Brockris and Potter, 1952; Bockris et al, 1957) next interesting phenomena was noticed: immediately upon application of voltage to an electrochemical system, a high but short-lived current spike was observed. When the applied voltage was disconnected, significant current continues to flow for a short time. In 1984 Ghoroghchian and Bockris designed a homopolar generator to drive an electrolyser on pulsed DC voltage. They concluded that the rate of hydrogen production would be nearly twice as much as the rate for DC.

The Latvian Hydrogen Research Team is developing inductive pulse power circuits for water electrolysis cell (Vanags et al, 2009, 2011a, 2011b). The studies revealed a few significant differences compared to conventional DC electrolysis of water. New model is established and described, as well as the hypothesis is set that water molecule can split into hydrogen and oxygen on a single electrode (Vanags et al, 2011a). There has been found and explained the principle of high efficiency electrolysis. A new type of power supply scheme based on inductive voltage pulse generator is designed for water electrolysis. Gases released in electrolysis process from electrodes for the first time are analyzed quantitatively and qualitatively using microsensors (dissolved gases in electrolyte solution nearby electrode) and mass spectrometer (in atmosphere evolved gases). The hypothesis of hydrogen and oxygen evolution on a cathode during the process of pulse electrolysis is original, as well as interpretation of the process with relaxation mechanisms of electrons emitted by cathode and solvated in electrolyte (Vanags, 2011b).

2. Literature review

2.1. A brief history of the electrolysis of water

Adriaan Paets van Troostwijk, 1752.–1837., and Johan Rudolph Deiman, 1743.–1808., while using Leyden jar and a powerful electrostatic generator noticed a gas evolution on the electrodes of water electrolysis cell as a result of spark over jumping in the electrostatic generator. The evolved gases displaced water out of the Leyden jar during the experiment and spark jumped into the collected gas mixture creating an explosion. The researchers decided that they have decomposed water into hydrogen and oxygen in a stoichiometric

proportion 2:1; they published the results in 1789, which is considered to be the year of discovering the water electrolysis (Zoulias et al, 2002; De Levie, 1999). In more that hundred years, in 1902 there were more than 400 industrial electrolyzers used all over the world, but in 1939 the first large water electrolysis plant was commissioned with the hydrogen production capacity of 10000 Nm³/h (Zoulias et al, 2002). The high-pressure electrolyzers were produced in 1948 for the first time; in 1966 General Electric built the first electrolysis system with solid electrolyte and in 1972 the first solid oxide high-temperature electrolyser was built. However the development of electrolysis devices is in progress nowadays as well along with the development of proton exchange membrane, which can be used in the water electrolyzers and fuel cells, along with the development of high-temperature solid oxide electrolyzers likewise the optimization of alkaline electrolyzers (Kreuter W, and Hofmann H (1998).

2.2. Direct current water electrolysis

When dissolving acid in the water (e.g. sulfuric acid), molecules of water and acid dissociate into ions. The same happens if alkali (e.g. KOH) is dissolved in the water, the solution dissociates into ions, creating ionic conductor or electrolyte. There has been formed an ionic conductor, where a direct current will be passed through. The processes taking place on electrodes are in the case of sulfuric acid - the positive hydroxonium ions H₃O⁺ (cation) move to the side of negative electrode. When cations reach the electrode, they receive missing electrons (Zoulias et al, 2002):



Hydrogen is produced as gas from the medium, in its turn, water dissociates into ions again. The reaction on an anode or positive electrode in an alkaline medium is (Zoulias et al, 2002):



Oxygen evolves as gas, but water dissociates into ions again. There are produced three parts of volume of gaseous substance in the process described - two parts of hydrogen and one - oxygen. In the case of alkaline electrolyte there are polarized water molecules, which have their hydrogen atoms oriented toward an electrode, near the cathode and dissociation reaction takes place:



The first law of thermodynamics for the open system states that:

$$Q - W_s = \Delta H \quad (4)$$

where Q is the amount of heat supplied to the system, W_s the amount of appropriate work performed by the system and ΔH is the change in system's enthalpy. The work done is electricity used up in electrolyser, therefore W_s is:

$$W_s = -nFE \quad (5)$$

where:

n - The amount of transferred electrons;

F - Faraday constant: = 23,074 cal/volts-g-equivalent;

E - Electric potential of the cell in volts.

Using equation (5), transform the expression (4), resulting:

$$E = \frac{\Delta H - Q}{nF} \quad (6)$$

In an isothermal reversible process (without loss) Q is:

$$Q_{atg} = T\Delta S \quad (7)$$

where T is absolute temperature and ΔS is system entropy change. From (6) and (7) the value of reversible reaction potential is obtained, where it is impossible to decompose water into hydrogen and oxygen in real time:

$$E_{rev} = \frac{\Delta H - T\Delta S}{nF} \quad (8)$$

$(\Delta H - T\Delta S)$ is the change in Gibbs free energy ΔG . At normal temperature and pressure ((25 °C temperature and 1 atm pressure) ΔH equals 68 320 cal/gmol and ΔG equals 56 690 cal/gmol. Therefore the reversible potential of the cell is:

$$E_{rev} = \frac{\Delta G}{nF} = \frac{56,690}{2(23,074)} = 1,23V \quad (9)$$

Potential where Q equals zero and supplied energy transforms into chemical energy, is called thermo-neutral voltage (Oldham and Myland, 1993; Bockris and Potter, 1952):

$$E_{thermo} = \frac{\Delta H}{nF} = 1,48V \quad (10)$$

The voltage to split water in practical electrolysis devices is higher than thermo-neutral cell voltage due transformation into heat, which heats up the cell. Therefore industrial electrolyser requires additional cooling and the value of DC voltage is defined:

$$E = E_{rev} + \text{loss} \quad (11)$$

where the

$$\text{loss} = E_{anode} + E_{cathode} + E_{mt} + IR \quad (12)$$

In equation (12) E_{anode} - activation overvoltage of the anode; $E_{cathode}$ - activation overvoltage of the cathode; E_{mt} - overvoltage of the mass transfer and IR - ohmic overvoltage (includes resistance in an electrolyte, on electrodes, leads). Current density must be higher than 100

mA/cm² in industrial electrolyzers, therefore voltage applied to individual cell partly transforms into the heat, becoming typical loss in DC water electrolysis.

It is possible to write an expression for the efficiency factor of the water electrolysis, calculated versus the thermo-neutral voltage, using relations above (Bockris and Potter, (1952):

$$\eta = \frac{\Delta H}{\Delta G + \text{loss}} = \frac{E_{\text{thermo}}}{E} \quad (13)$$

When ΔG is negative, the reactions are spontaneous and work has been done by releasing the energy. When ΔG is positive, for reaction to happen external work must be used. As for ensuring the reaction, work must be done, water electrolysis cell does not operate spontaneously. The reaction in fuel cells is spontaneous because of the catalyst and during reaction the energy is released (Salem, 2004).

Hydrogen Evolution Reaction (HER) is one of the most widely researched reactions in the electrochemistry. The studies of HER are carried out in different kind of systems and following each other processes is divided (Salem, 2004; Heyrovsky, 2006; Murphy, 1983; Bockris, 1957; El-Meligi, 2009; Sasaki and Matsuda, 1981; Noel and Vasu, 1990; Kristalik, 1965): Volmer electrochemical discharge step, Heyrovsky electrochemical desorption step, Tafel catalytic recombination step. Each of steps can be a reaction limiting step in a certain system during the whole reaction. This means, that each step can have different reaction rate, and the slowest step will determine the speed of reaction. Charge transfer may begin when the reagent is next to the electrode. Two most typical steps are charge transfer ending with the adsorption of hydrogen atom, and recombination of the adsorbed atoms with next desorption of H₂ molecule.

The general equation of the electrochemical reaction links current with potential (Noel and Vasu, 1990):

$$i_c = \bar{i} - \bar{i} = i_0 \left[\exp\left(-\frac{\beta\lambda\eta F}{RT}\right) - \exp\left(\frac{(1-\beta)\lambda\eta F}{RT}\right) \right] \quad (14)$$

β is symmetry factor (0, 1/2, 1 for process without activation, normal process and barrier-free process accordingly).

2.3. Interface between electrode and electrolyte: double layer

When two equal electrodes (conductors) are immersed in an electrolyte, initially there is no measurable voltage between them. But when the current is caused to flow from one rod to the other by a battery, charge separation is naturally created at each liquid/solid interface and two electrochemical capacitors connected in series are created. Typical capacitors store electrical charge physically, with no chemical or phase changes taking place, and this process is highly reversible; the discharge-charge cycle can be repeated over and over again, virtually without limit. In electrochemical capacitor at electrode/electrolyte interface solvated ions in the electrolyte are attracted to the electrode surface by an equal but opposite

charge in it. These two parallel regions of charges at interface form the “double layer” where charge separation is measured in molecular dimensions (i.e., few angstroms), and the surface area is measured in thousands of square meters per gram of electrode material (Miller and Simon, 2008).

Double-layer phenomena and electro-kinetic processes are the main elements of electrochemistry. It is considered that the behavior of the interface is and should be described in terms of a capacitor. It is a consequence of the “free charge” approach that in the case of a continuous current flow through the interface a strict distinction should be made between the so-called non-Faraday and Faraday currents. The former is responsible for charging of the double-layer capacitor, while the latter is the charge flow connected with the charge transfer processes occurring at the interface (Horányi, Láng, 2006). The state of an interface at constant pressure and temperature can be changed by changing the concentration of the components in the bulk phases, and by constructing an electrical circuit with the aid of a counter electrode and forcing an electric current through the circuit, which can be expressed as:

$$i = i' + i'' \quad (15)$$

Where i' is charging current of double layer, and i'' – charge transfer or Faraday current. Double layer charging current can be viewed as an ideal capacitor charging current equal to $C \frac{\partial \eta}{\partial t}$, where η is overvoltage and C – double layer capacitance. Rewriting equation (15), next current equation is obtained:

$$i = C \frac{\partial \eta}{\partial t} + i'' \quad (16)$$

which has caused much debates. Paul Delahais wrote in 1966 that this equation permits the decoupling of the non-Faraday from Faraday processes, but at the same time concludes that Faraday charge transfer and charging processes cannot be separated a priori in non-steady-state electrode processes because of the phenomenon of charge separation or recombination at the electrode-electrolyte interface without flow of external current. Charging behaviors as ideal polarized or reversible electrode represent only two limiting cases of a more general case (Delahay, 1966). Nisancioglu and Newman (2012) in their article even without going into the assumptions and basing only on the mass balance equation, obtained next current equation: $i = dq/dt + i''$ and showed that a priori separation of double-layer charging and Faraday processes in electrode reactions is the component mass balance for the electrode surface. Equation (1) is valid if the rate of change of concentration of the species, which take part in the electrode reaction, can be neglected at the electrode surface.

2.4. Water splitting with the pulse electrolysis

There are different ways of water splitting first reviewed by Bockris et al (1985), that sharply differs from conventional DC water electrolysis. The most common could be:

thermo chemical, sonochemical, photocatalytic, biological water splitting; water splitting under the magnetic field and centrifugal force of rotation; pulse electrolysis and plasma electrolysis. Regarding pulse electrolysis, Ghoroghchian and Bockris in 1956 already defined that the pulse electrolysis is more effective than conventional electrolysis. Many new patents on pulse electrolysis appeared in 1970-1990 (Horvath, 1976; Spirig, 1978; Themu, 1980; Puharich, 1983; Meyer, 1986; Meyer, 1989; Meyer, 1992a, 1992b; Santilli, 2001; Chambers, 2002) stating to be invented over-effective electrolysis (i.e. the current efficiency is higher than 100%). The water splitting scheme described in these patents initiated a huge interest, but nobody has succeeded in interpreting these schemes and their performance mechanisms up to now, and what is more important, nobody has succeeded to repeated patented devices experimentally as well.

In interrupted DC electrolysis the diffusion layer at the electrode can be divided into two parts: one part, which is located at the electrode surface is characterized with pulsed concentration of active ions, and another part is fixed, similar to the diffusion layer in case of DC. The concentration of the active ions in pulsing diffusion layer changes from defined initial value when the pulse is imposed, to a next value when it expired. The concentration of active ions in pulse may fall or can not fall to zero. Time, which is necessary for active ion concentration would fall to zero, is called the transition time τ . The transition time is depending from pulse current i_p and pulse duration T . If depletion in stationary diffusion layer is small, i.e. $c'_e \approx c_0$, where c'_e is concentration of ions in pulsed-layer outer edge, and c_0 is bulk concentration, the transition time can be found from Sand equation (Bott, 2000):

$$\tau = \frac{\pi D c_0^2 (zF)^2}{4i_p^2} \quad (17)$$

where F is Faraday's constant, z – charge number and D is its diffusion coefficient. As can be seen, transition time τ depends on the ion concentration in bulk volume c_0 and pulse current density i_p . Thickness of pulsed layer δ_p at the end of the pulse depends only from the density of pulse current:

$$\delta_p = 2 \left(\frac{DT}{\pi} \right)^{1/2} \quad (18)$$

With very short pulses extremely thin pulsating layer can be reached. This thin layer would allow temporary to impose a very high current densities during metal plating (more than 250A/cm², which is 10,000 times higher than currents in conventional electrolysis), which accelerates the process of metal electroplating (Ibl et al, 1978). The rough and porous surface is formed during metal plating with direct current, when the current value reached the mass transport limit. When plating is done with pulse current, pulsating diffusion layer always will be much thinner than the surface roughness, what means that in case the mass transfer limit is reached, the plated surface is homogeneous still and copy the roughness of substrate. This feature gives preference to pulse current in metal plating processes, comparing with conventional DC plating, because the highest possible power can be used (current above mass transfer limit) to obtain homogeneous coatings in shortest times (Ibl et al, 1978).

Pulse electrolysis is widely investigated using various technologies (Hirato et al, 2003; Kuroda et al, 2007; Chandrasekar et al, 2008). In all of these technologies rectangular pulses are mostly used which have to be active in nature. Shimizu et al (2006) applied inductive voltage pulses to water electrolysis and showed significant differences with conventional DC electrolysis of water. The conclusion of this research is that this kind of water electrolysis efficiency is not dependant on the electrolysis power, thus being in contradiction to the conventional opinion of electrolysis.

We studied inductive voltage electrolysis and promoted the hypothesis that pulse process separates the cell geometric capacitance and double layer charging current from the electrochemical reaction current with charge transfer (Vanags (2009), Vanags (2011a, 2011b). To prove this we have done plenty of experiments proving double layer charging process separation from the electrochemical water splitting reaction. There are no studies about the usage of reactive short voltage pulse in the aqueous solution electrolysis; also no microelectrodes are used to determine the presence of the dissolved hydrogen and oxygen near the cathode in electrolysis process.

3. Experimental

3.1. Materials and equipment

Materials, instruments and equipment used in this work are collected in Tables 1 and 2.

3.2. Inductive reverse voltage pulse generator

The inductive voltage pulses were generated in the electric circuit (Fig. 1) consisting of a pulse generator, a DC power source, a field transistor BUZ350, and a blocking diode (Shaaban, 1994; Smimizu et al, 2006). A special broad-band transformer was bifilarly wound using two wires twisted together. Square pulses from the generator were applied to the field transistor connected in series with the DC power source. The filling factor of pulses was kept constant (50%). To obtain inductive reverse voltage pulses, the primary winding of the transformer is powered with low amplitude square voltage pulses. In the secondary winding (winding ratio 1:1) due to collapse of the magnetic field induced in the coil very sharp inductive pulse with high amplitude and opposite polarity with respect to applied voltage appears. Pulse of induced reverse voltage is passed through the blocking diode, and the resulting $\sim 1 \mu\text{s}$ wide high-voltage pulse is applied to the electrolytic cell. A two-beam oscilloscope GWinstek GDS-2204 was employed to record the voltage (i.e. its drop on a reference resistance) and current in the circuit.

MOSFET (IRF840) is used as semiconductor switch between DC power supply and ground circuit. Pulse transformer is a solenoid type with bifilar windings; length is 20 cm and a coil diameter of 2.3 cm and ferrite rod core. Number of turns in both the primary and the secondary winding is 75, so ratio is 1:1. Inductance of solenoid is approximately $250 \mu\text{H}$. Super-fast blocking diode with the closing time of 10 ns is included in the secondary circuit, to pass on electrolysis cell only the pulses induced in transformer with opposite polarity. Direct pulses are blocked by diode.

	No	Name	Parameters	Producer
Chemicals	1.	KOH	99%	Aldrich
	2.	NaOH	99%	Aldrich
	3.	LiOH	99.9%	Aldrich
	4.	K ₂ CO ₃	99.8%	Aldrich
	5.	H ₂ SO ₄	95%	Aldrich
	6.	(NH ₂) ₂ CO	98%	Aldrich
	7.	H ₂ O	0.1 μS	Deionised
Metals	1.	Stainless Steel (parameters Table 2)		316L
	2.	Tungsten	95%	Aldrich
	3.	Platinum	99.9%	Aldrich
Equipments and Instruments	1.	DC power supply Agilent N5751A	300V; 2.5A	Aligent echnologies
	2.	Frequency Generator GFG-3015	0 – 150 MHz	GW-Instek
	3.	Oscilloscope GDS-2204	4 beams, resolution 10 ns	GW-Instek
	4.	Power Meter HM8115-2	16A, 300V	Hameg Instruments
	5.	Water Deionization Crystal – 5	Water - 0.1 μS	Adrona Lab.Systems
	6.	Masspectrometer RGAPro 100	0 – 100 m/z units	Hy-Energy
	7.	X-ray fluorescence spectrometer EDAX/Ametek, Eagle III		Ametek
	8.	Microsensors for dissolved gases H ₂ and O ₂	Resolution 0.1 μmol/l	Unisense, Denmark

Table 1. Materials and equipment used in this work.

Element	C	Si	P	S	Ti	Cr	Mn	Fe	Ni	Cu
Quantity, wt%	0.12	0.83	0.04	0.02	0.67	17.88	2.02	68.36	9.77	0.29

Table 2. Composition of Stainless steel 316L used for electrodes (wt%).

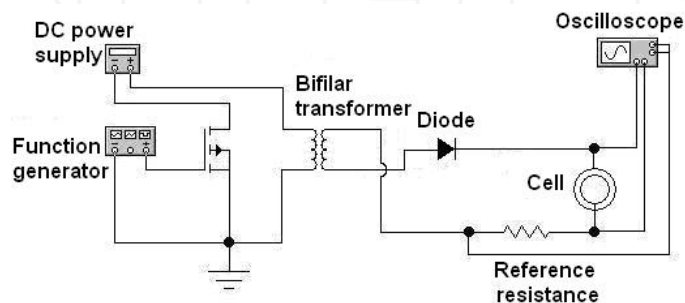


Figure 1. Experimental circuit for generation of inductive reverse voltage pulses.

3.3. Construction of electrolyses cells

Experiments in this chapter are divided into five parts. In the first part the gas evolution rate is explained and performance efficiency coefficients defined (current efficiency and energy efficiency). The second part examines kinetics of the inductive voltage pulse applied to electrolysis cell where electrolyte concentration and the distance between electrodes are changing. The third part describes the application of respiration microsensors to measure concentration of dissolved hydrogen gas directly to the cathode surface in an electrolysis cell, powered with inductive voltage pulses. The fourth experiment studied inductive voltage pulse kinetics in very dilute electrolyte solutions. The fourth experiment also noticed interesting feature in current pulse kinetics, therefore additional experiment is performed, to measure concentration of evolved hydrogen at the cathode with oxygen microsensor. This experiment devoted to fifth.

Amount of released gases during electrolysis was determined with volume displacement method (Fig. 2).

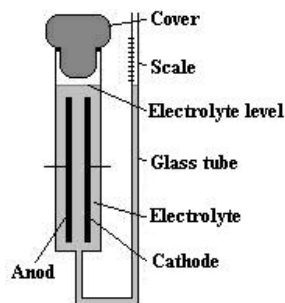


Figure 2. Principal scheme to determine the volume of released gases.

Electrolysis cell is in a separate chamber closed with a sealing cap. Glass tube bent in 180 degrees is attached to the bottom of the electrolysis chamber. The tube is graduated in units of volume above the level of the electrolyte. Gases arising in electrolysis process are pressing on electrolyte and the level in calibrated tube is increasing giving approximate volume of gases produced. In measured value of volume the 5% relative error is from different reasons; the biggest uncertainty is determined by the pressured gas generated during electrolysis - higher than atmospheric pressure. Gases are produced in electrolysis by volume 2/3 hydrogen and 1/3 oxygen. Knowing the mass of hydrogen generated in period t_{exp} , the charge necessary to produce such amount can be calculated and compared with consumed energy - result is current efficiency of particular electrolysis cell. Energy efficiency is calculated from consumed energy compared to what can be obtained from burning the produced amount of hydrogen at highest calorific value - 140 MJ/kg.

Self-made water electrolysis cell with movable electrode was used in experiments. It consists of a polyethylene shell with built in micro-screw from one side. Using stainless steel wire the micro-screw is connected to the movable electrode, situated perpendicular to the

electrolyte cavity (diameter 40 mm). Stainless steel stationary electrode with same area is situated against a moving electrode. SUS316L stainless steel plate electrodes with equal area (2 cm^2) were used in experiments. Before experiments the electrodes were mechanically polished and washed with acetone and deionized water. As an electrolyte KOH solution in water was used in different concentrations. At each electrolyte concentration the distance between electrodes was changed with micro-screw from 1 mm to 5 mm. During experiment the appropriate concentration of the electrolyte solution was filled and cell attached to an inductive voltage pulse generator. At each electrolyte concentration the current and voltage oscillograms were taken for 1 to 5 mm distance between electrodes (step 1 mm). Oscillograms were further analyzed calculating consumed charge, pulse energy, and in some cases - energetic factors.

To measure the concentration of dissolved hydrogen at the cathode during electrolysis, self-made cell was used (Fig. 3). Cell consists from three cameras connected with ion conducting bridges.

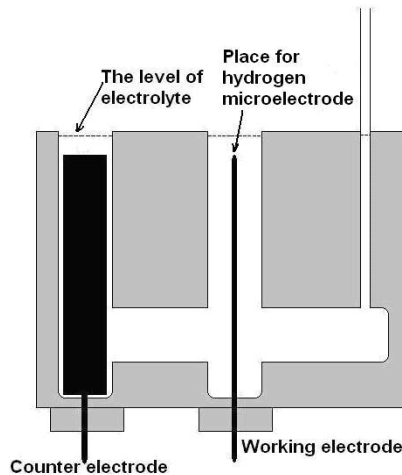


Figure 3. Three-camera electrolysis cell to measure concentration of dissolved hydrogen.

The first camera is for nickel plate counter electrode, second – for working electrode - smooth wires (diameter 0.5 mm, length 100 mm) of tungsten and platinum, but third camera was used for reference electrode in some specific experiments. Pt and W electrodes were cleaned before experiments, etching them 24 hours in concentrated alkali solution and rinsing with deionized water. The concentration of dissolved hydrogen was determined with respiration microsensor used typically in biological experiments (Unisense, 2011). The Unisense hydrogen microsensor is a miniaturized Clark-type hydrogen sensor with an internal reference electrode and a sensing anode. The sensor must be connected to a high-sensitivity picoammeter where the anode is polarized against the internal reference. Driven by the external partial pressure, hydrogen from the environment will pass through the sensor tip membrane and will be oxidized at the platinum anode surface. The picoammeter

converts the resulting oxidation current to a signal. In our experiments sensor H2100 having the tip with diameter $110\ \mu\text{m}$ was placed as closely as possible to cathode ($<1\ \text{mm}$ distance). Before experiments the microsensor was graduated in two points – zero H_2 concentration (Ar gas is bubbled through deionized water) and 100% or $816\ \text{mmol/l}$ at $20\ ^\circ\text{C}$ (H_2 gas is bubbled through deionized water – from Unisense, 2011 user manual). The experiment was carried out as follows: separate inductive voltage pulses was delivered to the cell and voltage and current oscillograms recorded. At the same time the concentration of the dissolved hydrogen was measured using microsensor.

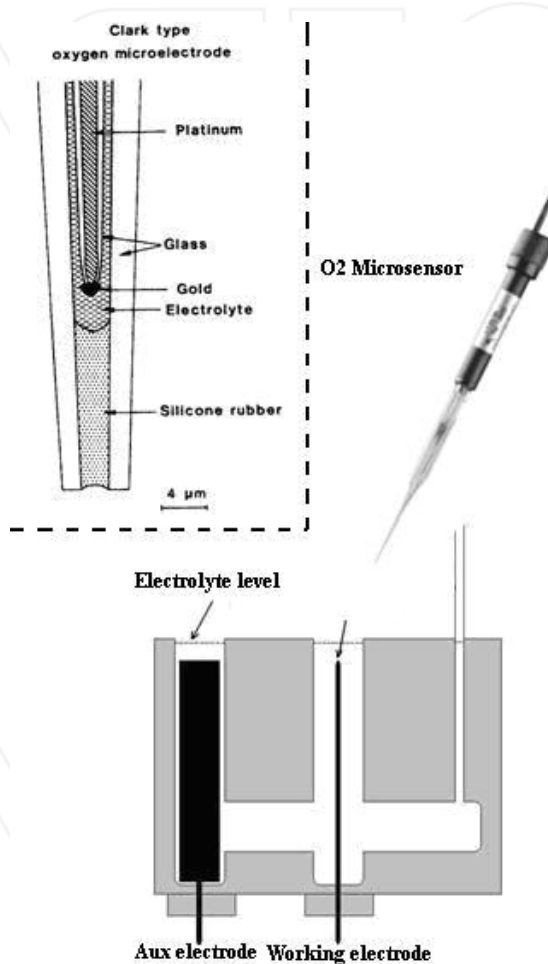


Figure 4. Water electrolysis cell to measure the concentration of dissolved oxygen.

The oxygen microsensor (also from Unisense, 2011) was used to measure the concentration of dissolved hydrogen close to cathode during inductive pulse electrolysis (Figure 4). The oxygen micro-sensor is all Clark-type sensor based on diffusion of oxygen through a silicone

membrane to an oxygen reducing cathode which is polarized versus an internal Ag/AgCl anode. The flow of electrons from the anode to the oxygen reducing cathode reflects linearly the oxygen partial pressure around the sensor tip (diameter $100\ \mu$) and is in the pA range. The current is measured by a picoammeter. To generate short inductive voltage pulses, the same circuit (chapter 3.2) is used. Cell is filled with deionized water, and the generator set in mode when expressed negative current peak is observed in oscillograms.

Concentration of oxygen is measured simultaneously with microsensor, previously calibrated in deionized water bubbled with oxygen.

Specific electrolysis cell was made for study the kinetics of inductive pulse electrolysis in diluted electrolytes (Figure 5). It was made from glass bowl with two separate electrode holders equipped with screws for electrodes from stainless steel 316L wires (diameter 2 mm, length 100 mm). Steel electrodes were cleaned before experiments, etching them 24 hours in concentrated alkali solution and rinsing with deionized water together with glass bowl of electrolysis cell. Very diluted electrolyte was prepared pouring in the cell 350 ml deionized water and adding drops of 5 M electrolyte from calibrated volume dropper ($0.05\pm 10\%$ ml). Four electrolytes (KOH, NaOH, LiOH, H_2SO_4) were used in experiments and measurements were registered after each drop.

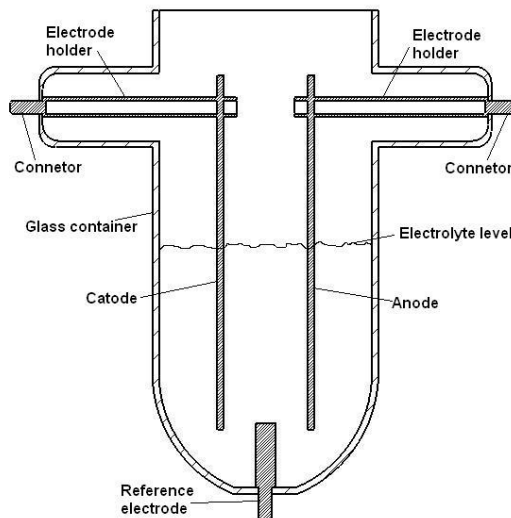


Figure 5. Water electrolysis cell to measure the kinetics of pulse electrolysis.

4. Results and analysis

4.1. Current and energy efficiencies

Average values of voltage and current, as well as flow of generated hydrogen gas depending on KOH concentrations are shown in table 3. Theoretically maximal current is

calculated knowing the hydrogen gas flow by assumption that 2 electrons generate one molecule of hydrogen. Using data from Table 3, current and energy efficiency coefficients are calculated for pulse electrolysis process (see Table 4) on the assumption that the pulse transformer primary side and secondary side are two separate systems, which are only bind by average value of current flowing in the cell.

KOH concentration [mol/kg]	Average value for current pulse [mA]	Average voltage value [V]	Current value calculated from mass of generated hydrogen [mA]	Hydrogen flow [cm ³ /min]
0.1	6.5	2.1	3.2	0.043
1	8	2.1	3.7	0.054
2	8.3	2.1	4	0.057
3	8.6	2.1	4.2	0.059

Table 3. Parameters of registered voltage and current pulses on an electrolysis cell.

This assumption is not entirely correct, but acceptable. When viewed from the primary circuit side, the pulse generator is with a reactive element included in its scheme - an induction coil (the primary winding of pulse transformer).

KOH concentration [mol/kg]	Current efficiency coefficient [%]	Energy efficiency coefficient [%]
0.1	49	66
1	46	64
2	48	68
3	49	68

Table 4. Current and energy efficiency coefficients

By disconnecting secondary side, primary side does not consume anything (except the power that is distributed on elements with active resistances included in the primary circuit). When connecting the secondary side, the active 1 V amplitude of the voltage pulse in the primary side is unable to consume more, because it is necessary to exceed electrolysis overvoltage – at least 1.23 V (ratio of windings in coil is 1:1).

Therefore, the average current values in Table 3 are replaced with the current consumed in the power supply system. Voltage value is read from the oscilloscope by measuring the voltage pulse on primary coil. Thus, equipment errors associated with variations in voltage values are excluded. Then, the resulting pulse is averaged over time and the resulting voltage values are shown in second column of Table 5.

It should be mentioned that adjusted energy efficiency coefficients were calculated without any reference to the circuit elements and the quantity of generated gas flow. As it is seen from Table 4.3., it is necessary to determine current and voltage values with oscilloscope within scheme of this experiment, which eliminates the pulse schemes for analogue measuring errors.

KOH concentration	Power supply voltage [V]	Average current value on the cell [mA]	Hydrogen flow [cm ³ /min]	Energy efficiency coefficient [%]
0.1	1.43	6.5	0.043	97
1	1.48	8	0.054	96
2	1.53	8.3	0.057	94
3	1.49	8.6	0.059	97

Table 5. Adjusted parameters of voltage, current and efficiency.

4.2. Pulse kinetics at different concentration solutions and electrode distances

In Figure 6 the voltage and current pulse oscillograms are shown for steel electrode plates in 0.1 M KOH solution, where the maximum voltage pulse value is approximately 5.5 V when distance between the electrodes is 5 mm and it drops to about 3 V when the distance between the electrodes is 1 mm. In 0.3 M KOH solution (curves similar to 0.1 M solution) the maximum voltage pulse value is 3.5 V, when distance between the electrodes is 5 mm and it drops to 2.6 V when distance between the electrodes is reduced to 1 mm. In even more concentrated solution, i.e., 0.5 M KOH, the maximum voltage pulse value at the electrode distance of 5 mm is approximately 2.9 V and when the electrode distance is 1 mm, it drops to 2.4 V. Current peak value does not change significantly depending on the electrode distance, or the concentration, but there are observed changes in the discharge tail length, suggesting that higher charge in electrolysis cell flows at more concentrated electrolyte solution.

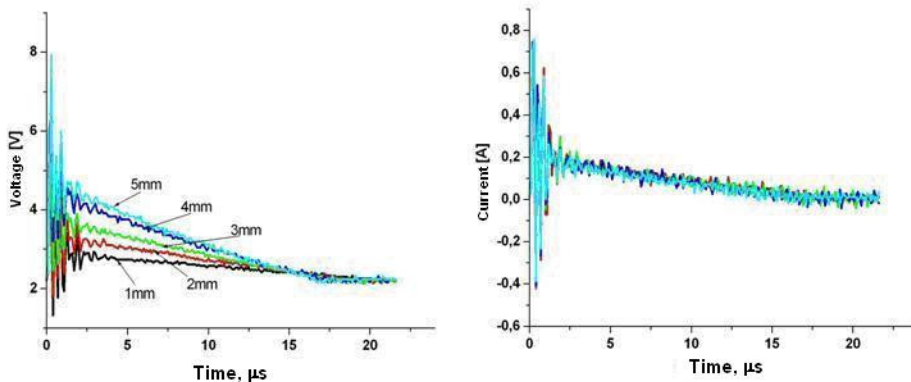


Figure 6. Current and voltage pulses registered with oscilloscope in 0.1 M KOH.

When looking at pulse generation scheme in the experimental method section (Figure 1), it is clear that high-voltage pulse generated in the transformer is reactive in nature. Reactive pulse amplitude will depend on the quality factor of capacitive element. Capacitor with a large leak (concentrated electrolyte solution) will not be able to hold the reactive pulse with large amplitude, though in the previous figures it is shown that the amplitude of those achieved in the secondary circuit on the electrolysis cell is greater than the direct pulse

amplitude. This means that at the first moment when short inductive pulse is applied, the water electrolysis cell behaves as good capacitor, also at the voltage region, in which water electrolysis can occur. But after starting the discharge tail, the energy stored in the capacity transforms into the chemical energy in the process of water electrolysis.

4.3. The concentration of dissolved hydrogen at cathode

Current and voltage pulses registered with oscilloscope (Fig. 7) show that changing the electrode material, the rising front and relaxation of voltage pulses does not change, while voltage pulse amplitude decreases with increasing current pulse amplitude when solution concentration increases. Current pulses also are not different on the platinum and tungsten electrodes with identical concentration of KOH solutions (Fig. 7). To evaluate pulse energy supplied to the cell, pulse voltage and current values were multiplied and resulting curves were integrated with time (Table 6). Each row in the Table 6 shows electrode material and the concentration of the solution, and in the next column – calculated supplied energy to the system during the pulse.

Figure 8 presents each electrode's voltage and current oscillograms in the same time scale in order to better evaluate the phase shift angle between current and voltage. There are not noticeably significant differences observable between the phase shift angles depending on the electrode material.

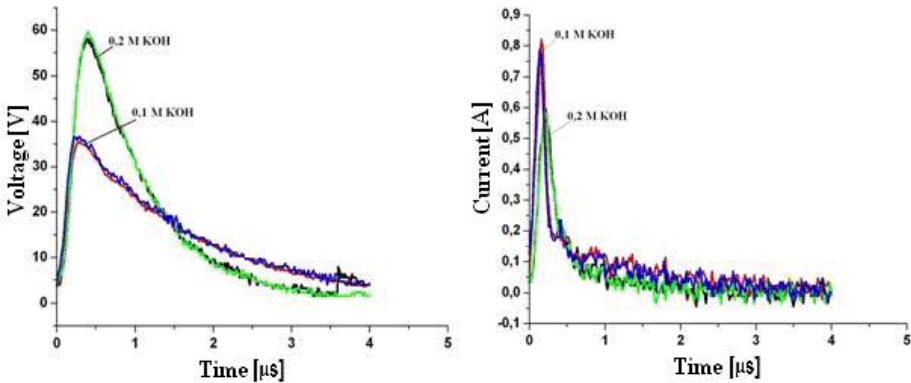


Figure 7. Current and voltage pulse oscillograms of Pt and W electrodes (Pt – black and blue, W – green and red accordingly).

Electrode material and solution concentration	Energy, mJ
Pt in 0.1M KOH solution	8.5
Pt in 0.2M KOH solution	7.7
W in 0.1M KOH solution	8.2
W in 0.2M KOH solution	7.6

Table 6. Energy supplied to the cell during the pulse, calculated from voltage and current oscillograms.

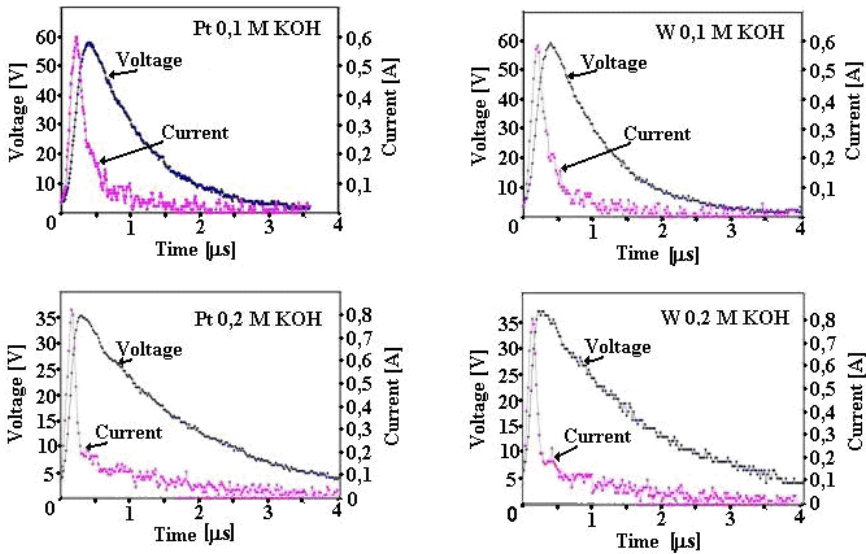


Figure 8. Current and voltage pulse oscillograms of Pt and W electrodes in 0.1 M and 0.2 M KOH

In each experiment with microsensor to measure the concentration of dissolved hydrogen, the measuring time lasted 100 s (curves at Fig. 9). As it is seen, the curves with largest slope are an electrolyte with a higher concentration, and the tungsten electrode, rather than platinum.

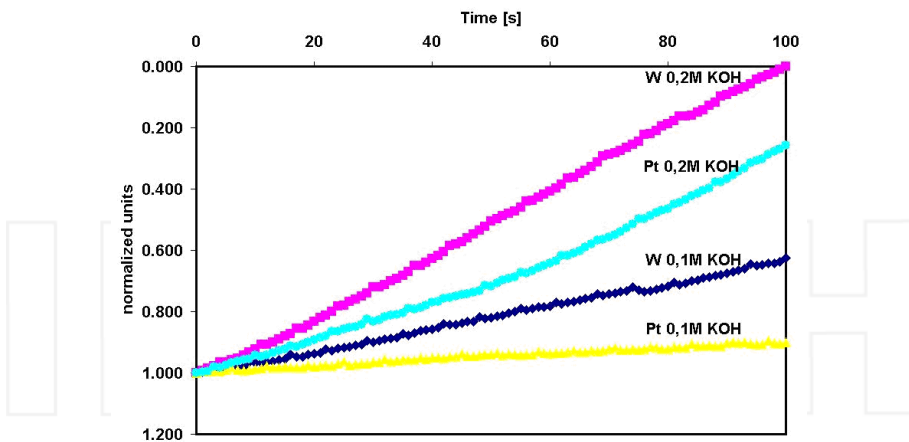


Figure 9. Changes in concentration of dissolved hydrogen gas during pulse electrolysis.

It means that on the tungsten electrodes the concentration of dissolved hydrogen increases faster than on the platinum electrodes. As it is seen from cathodic region of voltamperic curves (Fig. 10), for platinum electrode the characteristic hydrogen adsorption/absorption peak at negative currents appears at potential -0.5 V, but not for tungsten electrode.

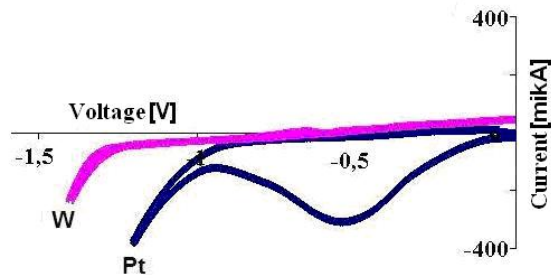


Figure 10. Voltamperic characteristics for platinum and tungsten electrodes in 0.1 M KOH solution measured in two electrode configuration at scan rate 10 mV/s.

The pulse energy of inductive reverse voltage pulses is limited. Voltage and current during the pulse reacts in such way that their multiplication and next integration in time would be equal in the same concentration of electrolyte without reference to the material of electrodes that are used. Pulse energy decreases whilst solution concentration increases, suggesting that reactive energy component has decreased. Therefore it is observable that phase shift angle between current and voltage is smaller in a more concentrated solution. Since the inductive voltage pulse energy is limited, on platinum electrode it is consumed in the adsorption area, thus structuring hydrogen adsorption monolayer on the platinum electrode. There is no hydrogen adsorption/absorption peak for tungsten electrode and during a very short voltage pulse, electrons from the metal discharge directly on hydrogen ions at interface electrode/electrolyte and hydrogen molecules are formed intensively which are detected with dissolved hydrogen microsensor.

4.4. Pulse kinetic measurements in highly dilute solutions

Voltage pulse growth at various concentrations of KOH solution (Figure 11) is equal in all concentrations, while the discharge tail after voltage pulse at various concentrations is different. Amplitude of voltage pulse is maximal in deionized water, but pulse dynamics in cell with slightly diluted electrolyte is exactly what is in the case of the open circuit, only the amplitude is smaller. Continuing to increase the concentration of electrolyte in cell, the value of voltage pulse amplitude continues decrease, while the discharge tail will increase.

Current changes the direction from negative to positive with increasing concentration of electrolyte passing through the point where the current pulse has not descending a long tail (Fig. 12). Current pulse in deionized water most of the momentum is negative. By increasing the concentration of solution up to 1 mM, current pulse appears in both positive and immediately following a negative pulse, while discharge tail almost disappears. Continuing to increase the concentration of electrolyte, the negative values of current pulse disappear and the discharge tail remains positive and increasing, which indicates that the charge injected in the cell during pulse increases. More increase of concentration does not change the view of current pulse and it remains like from the previous concentrations (Fig. 12).

When electrolyte concentration increases, voltage peak drop is observed (Fig. 13). The peak value of voltage pulse is decreasing exponentially, and it stabilizes around the value of 9 V for solutions, while in deionized water that value is over 600 V. These curves almost coincide in different alkali solutions, while in the sulfuric acid the peak values are falling faster.

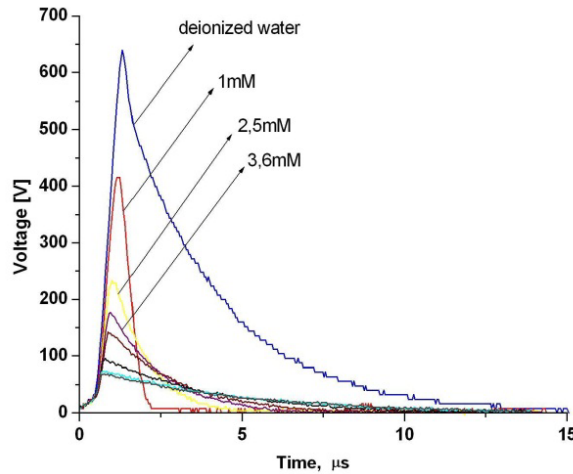


Figure 11. Inductive discharge voltage pulses with different concentrations of KOH.

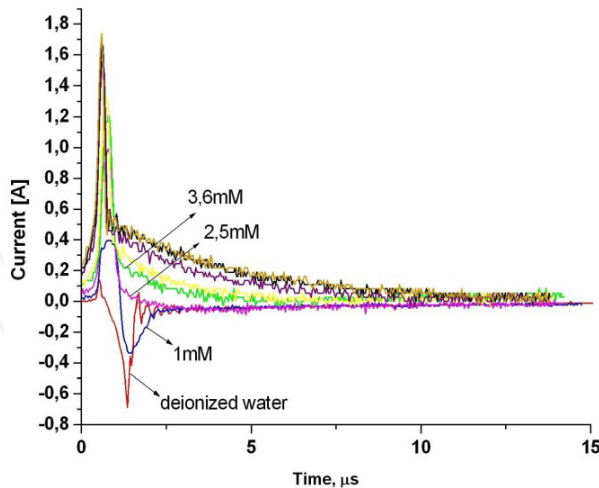


Figure 12. Current pulses initiated by inductive voltage pulses on cell with different concentrations of KOH solution

The pulse charge (integral of the current pulse) increases with increase of electrolyte concentration and tend saturate at some value (Figure 14).

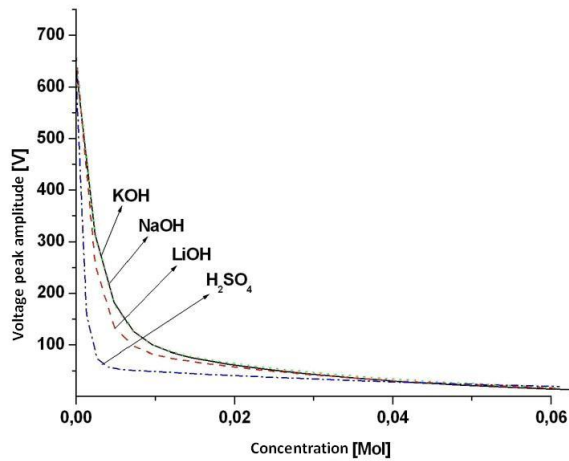


Figure 13. Decrease of voltage pulse amplitude with increasing concentration of electrolyte.

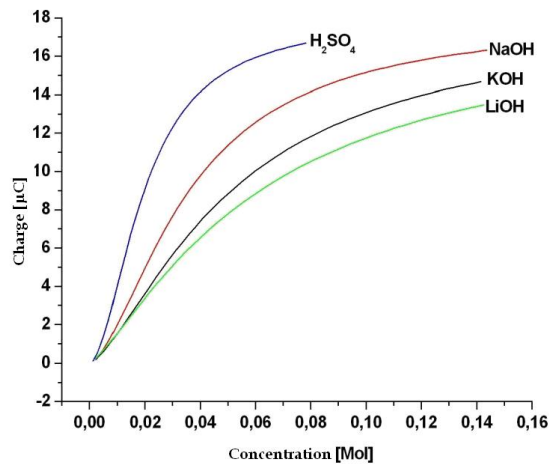


Figure 14. Changes of pulse charge (integrated current pulse) in various solutions with increasing concentration of electrolyte.

In alkali solutions, the charge behavior is nearly identical for alkali tested, while in the cell with sulfuric acid solution, the increase of charge is more rapid. Concerning occurrence of the negative currents following hypothesis is proposed. Voltage pulse kinetics demonstrates that around the electrode spatial charge density appears, i.e., when voltage rapidly grows in two-electrode system, electrons are emitted from the cathode environment. Since water ion concentrations in deionized water is low (H_3O^+ molar concentration is in the order of 10^{-7} M), then, most likely, the emitted electrons are solvated between polar water molecules and than will attach a neutral water molecule, which is described by following hydration reaction:



If OH^- ions and solvated electrons don't manage to discharge at the cathode, then around the cathode a spatial charge appears. In case of arising the spatial charge around electrode, it is more likely of electrons to move back into the metal. If the electron donor is the OH^- ion, then oxygen evolution should appear at the cathode. In principle, according to the experimental circuit, such electron returning back in metal in large amounts what results from the negative current pulse value presented in Fig. 12, is not possible since this current component is blocked by the diode incorporated in the circuit. Therefore behind the diode, parasitic element with the inductive nature must exist in the measurement circuit (Fig. 1) which becomes comparatively small and solvated electrons are discharged by ions in electrolyte, therefore decreasing negative current. To confirm this hypothesis, it is necessary to determine if oxygen does not appear near the cathode (the solvated electrons OH^- form allows a reverse reaction (19) on the cathode).

4.5. Measurement of dissolved oxygen near the cathode

The concentration of dissolved oxygen in a solution near the cathode during pulse electrolysis in dependence of time is presented in Fig. 15. During the first 60 seconds current pulses has an explicit negative peak in the cell. After 60 seconds, the generator is set to manage the negative current peak disappeared. From Fig. 15 it is seen that when a negative current peak occurs, the oxygen evolves at the cathode, but when the negative current during voltage pulses is prevented, the oxygen at cathode is no longer released and concentration decreases.

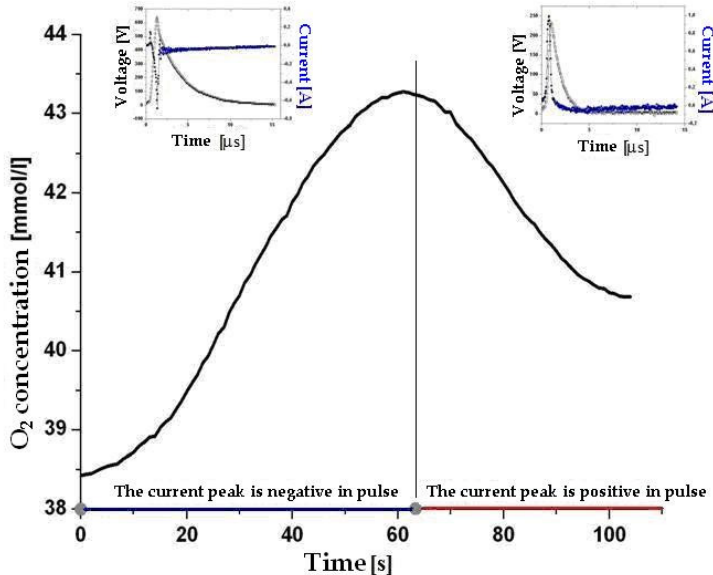


Figure 15. Dissolved oxygen concentration near the cathode in two regimes of pulse generator – when current peak is negative (left, dissolved oxygen concentration is increasing) and positive (right, dissolved oxygen concentration is decreasing).

5. Conclusions

Reactive short voltage pulse generator is designed to power water electrolysis cells of different constructions, both with spatially separated and with variable distance electrodes. Required value of electrolysis voltage in the primary circuit of power supply can be reduced by inserting the electrolysis cell in secondary circuit of power supply together with inductive element and reverse diode. For example, in this work electrolysis is provided with direct pulse amplitude 1 V, which induces a short high voltage pulse (tens, hundreds of volts, depending on the conductivity of electrolyte) in the secondary circuit. For studying the process of electrolysis the microelectrode sensors are used to measure concentration of dissolved hydrogen and oxygen gas in the direct vicinity of cathode for the first time.

By changing the distance between the electrodes and concentration of electrolyte, it is experimentally proved that the electrolysis cell is capacitor with high Q factor when short voltage pulse (width below 1 μ s) is applied. During this short time the capacitor (electrolysis cell) is charged, which can be interpreted as charging of double-layer on interface cathode/electrolyte. After the interruption of short voltage pulse the energy accumulated in double-layer capacitor slowly discharges (pulse discharge tail), thus activating the process of electrolysis. Consequently, it is shown that with short voltage pulse electrolysis the charging of cell can be separated from the electrochemical reactions in electrolysis process. Kinetics of charging the electrolysis cell with reactive high voltage short pulses does not depend on concentration of the electrolyte, whereas kinetics of the subsequent long-discharge process depends on the electrolyte concentration (faster in dilute solutions, slower in more concentrated solutions). If concentration of electrolyte in the electrolysis cell is above 3 mM, reactive voltage pulse energy does not depend on concentration of the solution. The current polarity switch from cathodic to anodic and back is observed in oscillograms, when de-ionized water electrolysis is performed with short reactive voltage pulses. Polarity changes only during short time when reactive voltage pulse is applied; at the beginning of the discharge tail the current is cathodic again. Measurements of dissolved oxygen concentration by microsensor in the immediate vicinity of the cathode show that oxygen concentration increases (reverse process to hydrogen evolution) in the presence of anodic current. The hypothesis is proposed that high-voltage pulse causes the emission of electrons from the cathode metal into electrolyte, where at first the electrons are solvated, then dissociating the water molecules forms H atoms and OH⁻ ions; next generated OH⁻ ions can discharge on cathode at the moment when applied voltage pulse reduces, giving the release of oxygen detected by microsensor. Current efficiency of 50% is registered in high-voltage reactive short pulse electrolysis, while the energetic efficiency is in range 70-100%.

Platinum and tungsten electrodes are studied to find the impact of electrode material on the process of short reactive voltage pulse electrolysis. Experimental results show that the voltage and current characteristics of inductive voltage short pulse electrolysis are the same

for both metals, but the concentration of dissolved hydrogen grows faster at the tungsten electrode. Delay in the release of hydrogen on a platinum electrode is explained by the tendency of platinum to adsorb hydrogen on the surface.

Author details

Martins Vanags, Janis Kleperis and Gunars Bajars
Institute of Solid State Physics, University of Latvia, Riga, Latvia

Acknowledgements

The authors acknowledge laboratory colleagues Liga Grinberga and Andrejs Lūsis for stimulating discussions, and Vladimirs Nemcevs for technical assistance. Authors thank Professor Robert Salem for helpful guidance and advices, and deep compassion to his family on the death of Professor in 2009. Financial support from the European Social Fund project "Support for doctoral studies at the University of Latvia" is acknowledged by M.Vanags. All authors thank the National Research Program in Energy supporting the development of hydrogen infrastructure in Latvia.

6. References

- Bockris O'M and Potter E.C. (1952) The mechanism of the Cathodic Hydrogen Evolution reaction, *Journal of the Electrochem. Society*, Vol. 99:169 – 186.
- Bockris J.O'M., Ammar I.A., Huq A.K.S. (1957). The Mechanism of the Hydrogen Evolution Reaction on Platinum, Silver and Tungsten surfaces in Acid Solutions. *J Chem Phys*, 61:879–886.
- Bockris J.O'M., Dandapani B., Cocke D. and Ghoroghchian J. (1985) On the Splitting of Water. *International J. Hydrogen Energy*, Vol. 10:179-201, 1985.
- Bott A.W. (2000) Controlled Current Techniques. *Current Separations* 18/4:125-127.
- Chambers, S.B. (2002) Method for producing orthohydrogen and/or parahydrogen. *US Patent 6419815* (2002).
- Chandrasekar M.S., Pushpavanam M. (2008) Pulse and pulse reverse plating—Conceptual, advantages and applications. *Electrochimica Acta*, 53:3313–3322.
- Delahay P. (1966) Electrode Processes without a Priori Separation of Double-Layer Charging, *The Journal of Physical Chemistry*, 70: 2373–2379.
- De Levie R (1999). The electrolyses of water. *Journal of Electroanalytical Chemistry* 476:92-93.
- Dimants J, Sloka B, Kleperis J, Klepere I (2011) Renewable Hydrogen Market Development: Forecasts and Opportunities for Latvia. Paper No 319GOV, Proceedings of *International Conference on Hydrogen Production ICH2P-11*, June 19-22, 2011, Thessaloniki, Greece, p.1-6

- El-Meligi A.A., Ismail N. (2009) Hydrogen evolution reaction of low carbon steel electrode in hydrochloric acid as a source for hydrogen production, *International Journal of Hydrogen Energy* 34:91 – 97.
- Ghoroghchian J., Bockris J.O'M. (1985) Use Of A Homopolar Generator In Hydrogen Production From Water, *International Journal of Hydrogen energy*, vol. 10:101-112.
- Gutmann F, Murphy O.J (1983) The Electrochemical Splitting of Water, In book: R.E. White, J.O'M. Bockris, B.E. Conway (Eds.), *Modern aspects of electrochemistry*, vol. 15, p. 1, Plenum, New York (1983) pp. 5–13
- Heyrovsky M (2006) Research Topic – Catalysis of Hydrogen Evolution on Mercury Electrodes, *Croatica Chemica Acta* 79 (1) (2006) 1-4
- Hirato T., Yamamoto Y., Awakura Y. (2003) A new surface modification process of steel by pulse electrolysis with asymmetric alternating potential. *Surface and Coatings Technology* 169/170:135–138.
- Horányi G., Láng G.G. (2006) Double-layer phenomena in electrochemistry: Controversial views on some fundamental notions related to electrified interfaces, *Journal of Colloid and Interface Science* 296:1–8.
- Horvath, St. (1976) Electrolysis apparatus. *US Patent 3954592* (1976).
- Hydrogen Pathway (2011). Welcome to the Roads2HyCom Hydrogen and Fuel Cell Wiki: Cost Analysis; 18.11.2011; Available from: www.ika.rwth-aachen.de/r2h/index
- Ibl N., Puippe J.Cl. and Angerer H. (1978) *Electrocrystallization in pulse electrolysis*. *Surface Technology*, 6:287 – 300.
- Kisis G., Zeps M., Vanags M. (2009) Parameters of an efficient electrolysis cell, *Latvian Journal of Physics and Technical Sciences*. Riga, 2009, N3. 6 p.
- Kreuter W, and Hofmann H (1998) Electrolysis: the important energy transformer in a world of sustainable energy, *Int. J. Hydrogen Energy* 23(8): 661-666.
- Kristalik L.I. (1965) Barrierless Electrode Process, *Russian Chemical Reviews*, Vol.34:785 – 793.
- Kuroda K., Shidu H., Ichino R. and Okido M. (2007) Osteoinductivity of Titania/Hydroxyapatite Composite Films Formed Using Pulse Electrolysis, *Materials Transactions*, 48:328-331.
- Meyer, S.A. (1986) Electric pulse generator. *US Patent 4613779* (1986).
- Meyer, S.A. (1989) Gas generator voltage control circuit. *US Patent 4798661* (1989).
- Meyer, S.A. (1992) Process and apparatus for the production of fuel gas and the enhanced release of thermal energy from such gas. *US Patent 5149407* (1992).
- Miller J.R. and Simon P. (2008) Fundamentals of Electrochemical Capacitor Design and Operation, *The Electrochemical Society Journal Interface*, Spring:31-32.
- Murphy G.F. (1983). In: White RE, Bockris JO'M, Conway BE, editors. *Modern aspects of electrochemistry*, vol. 15. NewYork: Plenum Press; 1983. p. 5-13
- Nisancioglu K. and Newman J. (2012) Separation of Double-Layer Charging and Faradaic Processes at Electrodes, *Journal of The Electrochemical Society*, 159:E59-E61.

- Noel M, Vasu K.I. (1990) *Cyclic Voltammetry and the Frontiers of Electrochemistry*, Oxford and IBH Publishing Co. Pvt. Ltd., New Delhi, 1990., 695 p., ISBN 81-204-0478-5.
- Oldham K.B., Myland J. C. (1993) *Fundamentals of Electrochemical Science*, United Kingdom: Academic Press Limited, 1993, 474 p.
- Our Common Future* (1987) Book, Oxford: Oxford University Press. ISBN 0-19-282080-X
- Puharich, H.K. (1983) Method & Apparatus for Splitting Water Molecules. *US Patent 4,394,230* (1983).
- Salem R. R.(2004) *Chemical Thermodynamics*, Fizmatlit, 2004., 352 p, ISBN 5-9221-0078-5
- Santilli, R.M. (2001) Durable and efficient equipment for the production of a combustible and non-pollutant gas from underwater arcs and method therefore. *US Patent 6183604* (2001).
- Sasaki T., Matsuda A. (1981) Mechanism of Hydrogen Evolution Reaction on Gold in Aqueous Sulfuric Acid and Sodium Hydroxide, *J. Res. Inst. Catalysis*, Hokkaido Univ., Vol. 29:113 – 132.
- Selected Articles of Hydrogen Phenomena* The Book, Editors: T. Nejat Vezgöğlü, M. Oktay Alniak, Ğenay Yalçin; 1.Basım: Ekim 2009, ISBN: 978-605-5936-23-5, p. 39-45.
- Shaaban A.H. (1994) Pulsed DC and Anode Depolarisation in Water Electrolysis for Hydrogen Generation, HQ Air Force Civil Engineering Support Agency Final Report, August, 1994. 21.11.2011. Available from: <http://www.free-energy-info.co.uk/P1.pdf>
- Shimizu N., Hotta S., Sekiya T. and Oda O. (2006) A novel method of hydrogen generation by water electrolysis using an ultra-short-pulse power supply. *Journal of Applied Electrochemistry*, 36:419–423.
- Spirig, E. (1978) Water decomposing apparatus. *US Patent 4113601* (1978).
- The Hydrogen Economy (2004): Opportunities, Costs, Barriers, and R&D Needs. 21.11.2011; Available from: http://www.nap.edu/openbook.php?record_id=10922&page=R1
- Themu, C.D. (1980) High voltage electrolytic cell. *US Patent 4316787* (1980).
- Unisense Microsensors (2011). Tool Guide 15.11.2011. From: UNISCIENCE Science: Available from: <http://www.unisense.com/Default.aspx?ID=458>; <http://www.unisense.com/Default.aspx?ID=443>
- Vanags M, Shipkovs P, Kleperis J, Bajars G, Lusiš A (2009) Water Electrolyses – Unconventional Aspects” In Book: *Selected Articles Of Hydrogen Phenomena*. Editors: T. Nejat Vezgöğlü, M. Oktay Alniak, Ğenay Yalçin; 1.Basım: Ekim 2009, ISBN: 978-605-5936-23-5, p. 39-45.
- Vanags M, Kleperis J and Bajars G (2011a) Electrolyses Model Development for Metal/Electrolyte Interface: Testing with Microrespiration Sensors. *International Journal of Hydrogen Energy*, vol. 36:1316-1320.
- Vanags M, Kleperis J and Bajars G (2011b) Separation of Charging and Charge Transition Currents with Inductive Voltage Pulses. *Latvian Journal of Physics and Technical Sciences*, No 3, p. 34-40.

Zoulias E., Varkaraki E., Lymberopoulos N., Christodoulou C.N. and Karagiorgis G.N. (2002) A Review On Water Electrolysis. Centre for Renewable Energy Sources (CRES), Pikermi, Greece. 21.11.2011. Available from: <http://www.cres.gr/kape/publications/papers/dimosieyseis/ydrogen/A%20REVIEW%20ON%20WATER%20ELECTROLYSIS.pdf>

INTECH

INTECH